Biosensors and Bioelectronics 52 (2014) 196–201

Contents lists available at ScienceDirect

Biosensors and Bioelectronics

journal homepage: www.elsevier.com/locate/bios

Glad assisted synthesis of NiO nanorods for realization of enzymatic reagentless urea biosensor

Manisha Tyagi [a], Monika Tomar [b], Vinay Gupta [a,*]

[a] Department of Physics and Astrophysics, University of Delhi, Delhi 110007, India
[b] Physics Department, Miranda House, University of Delhi, Delhi 110007, India

ARTICLE INFO

Article history:
Received 3 July 2013
Accepted 13 August 2013
Available online 29 August 2013

Keywords:
NiO nanorods
GLAD
Urea
Biosensor

ABSTRACT

NiO nanorods (Nr-NiO) synthesized under glancing angle deposition (GLAD) configuration in RF sputtering have been explored for potential application in urea biosensor. Vertically aligned cone shaped NiO nanorods synthesized over ITO coated glass (Nr-NiO/ITO/Glass) exhibit enhanced electrochemical current in a reagent less buffer due to its electro-catalytic species that are based on the shuttling of electrons between Ni^{2+} and Ni^{3+} in the octahedral site. The fabricated bioelectrode (Ur/Nr-NiO/ITO/glass) after immobilization of urease (Ur) shows excellent biosensing response characteristics with a relatively high sensitivity of about 48.0 μA/(mM) and a good linearity over a wide range (0.83–16.65 Mm) of urea concentration with the long shelf life of about 20 weeks. The low value of the Michaelis–Menten constant (K_m=0.47 mM) indicates the high affinity of immobilized urease (Ur) towards the analyte (urea). The high electro-catalytic activity, along with the redox behavior of Nr-NiO, makes it an efficient matrix for the realization of a reagent less urea biosensor.

1. Introduction

Urea [$(NH_2)_2CO$] is an important metabolite, dissolved in human physiological fluids whose appropriate level (1.33–3.33 mM) is very important. Its disturbed level is an indicator of numerous metabolic disorders including renal failure (acute or chronic), urinary tract obstruction, dehydration, shock, burns and gastrointestinal bleeding related to hyper concentration of urea and on the other hand hypo-concentrations of urea in human beings is related to hepatic failure, nephritic syndrome, cachexia (low-protein and high-carbohydrate diets), etc. (Ansari et al., 2009; Saipina et al., 2011; Lakard et al., 2011; Krawczyk et al., 2000). Hence, it is of utmost interest to develop cost-effective techniques for real-time monitoring of urea. Urease hydrolysis the urea liberating NH^{4+} and HCO^{3-} ions which can be detected by a number of transducers including amperometric, potentiometric, optical, thermal, and piezoelectric (Ansari et al., 2009; Ahuja et al., 2011; Knock et al., 2001; Yang et al., 2007). Concentration of librated NH^{4+} and HCO^{3-} ions is directly related to the concentration of urea. A comparison was made between the amperometric and potentiometric transducers used for the analysis of urea and it was reported that the amperometric biosensors were better as the potentiometric biosensors suffered from the interference from potassium and sodium ions (Dhawan et al., 2009). Enzyme-based amperometric biosensor is the most promising approach since it depends on the shuttling of electron from the electrolyte to the electrode and offers low detection limit, high sensitivity, high selectivity with high shelf life (Dhawan et al., 2009). Response time of such biosensors is directly associated with the hydrolysis rate of urea on the electrode surface; therefore, rapid production of NH^{4+} ions on the electrode surface will lead to a highly sensitive biosensor. Hence, for obtaining enhanced biosensing response characteristics, choice of an appropriate electrode having suitable matrix is important. Several matrices based on conducting polymers, CNTs, metals, metal oxides, etc., have been used to immobilize urease for the fabrication of urea biosensors (Bozgeyik et al., 2011; Tiwari et al., 2009; Gabrovska et al., 2011; Chirizzi et al., 2011). Recently, nanostructured matrices are being explored extensively by the research community for biosensing applications since they provide high surface-to-volume ratio for efficient loading of enzyme (Chirizzi et al., 2011; Das et al., 2010; Kaushik et al., 2009; Ali et al., 2009). However, nanostructures are in general, fabricated by chemical route like sol–gel, electrodeposition, chemical vapor deposition etc. and have been suffering with the problem of fast degradation in biosensing response characteristics with time and thus limits their application for in vivo-monitoring (Bozgeyik et al., 2011; Tiwari et al., 2009; Gabrovska et al., 2011; Kaushik et al., 2009; Ali et al., 2009; Velichkova et al., 2011). Jia et al. (2011) reported the detection of urea using hybrid polyaniline

* Corresponding author. Tel.: +91 9811563101.
E-mail addresses: drguptavinay@gmail.com, drvin_gupta@rediffmail.com (V. Gupta).

0956-5663/$ - see front matter © 2013 Elsevier B.V. All rights reserved.
http://dx.doi.org/10.1016/j.bios.2013.08.020

(PANi) nanofibers with integrated Pt nanoflowers but the sensitivity of the developed biosensor was very low (0.11 μA mM^{-1}). Bozgeyik et al., developed the amperometric urea biosensor based on nanostructured polymer membrane and reported that the sensitivity degraded by 49% in just 10 days. Metal oxides are reported to be advantageous over other matrices for biosensing application (Tyagi et al., 2012; Batra et al., 2012; Solanki et al., 2008). However, little attention has been given towards utilization of metal oxide nanostructures prepared by physical deposition techniques besides the fact that reproducible growth with controlled morphology may be advantageous for obtaining high sensitivity and shelf life. Ali et al., (2009) and Kaushik et al. (2009), fabricated amperometric urea biosensors based on metal oxide nanostructured matrix, but low sensitivity (< 10 μA mM^{-1}) with small shelf life was observed.

Amongst the metal oxide matrices, nickel oxide (NiO), due to its high electrocatalytic properties, good oxygen ion conductivity, biocompatibility, nontoxicity, high chemical stability, and fast electron transfer feature, is a promising candidate for the development of biosensors (Arora et al., 2011; Li et al., 2008). The high isoelectric point (IEP = 10.7) of NiO is also advantageous for immobilization of biomolecules having low IEP like urease via strong electrostatic interaction. NiO thin films and their composites have been efficiently used for detection of various biomolecules including hemoglobin, glucose, metformin, uric acid and sulfide in desired test specimens (Arora et al., 2011; Li et al., 2008; Zang et al., 2010; Sattarahmady et al., 2010). In our earlier work, NiO nanoparticles synthesized using chemical route were utilized for realizing urea biosensor using external reagent in the PBS buffer, where the shelf life of the bioelectrode degraded up to 16% after 20 weeks (Tyagi et al., 2013). However, no efforts have been made towards the growth of NiO nanorods especially using reproducible physical deposition technique such as RF sputtering for the fabrication of an enzymatic reagent less urea biosensor. In the present work, a novel method of synthesizing conical shaped NiO nanorods using RF magnetron sputtering technique under glancing angle deposition (GLAD) configuration is employed. The array of NiO nanorods are fabricated on the ITO coated glass slide for the development of an efficient and reagentless amperometric urea biosensor.

2. Experimental

2.1. Materials

Urease (Ur) (from jack beans) and potassium iodide were purchased from Sigma-Aldrich. Sodium phosphate monobasic anhydrous and sodium phosphate dibasic dihydrate were obtained from Sisco Chemical, India. All chemicals were used without further purification. deionised (DI) water (resistivity = 18.2 MΩ cm^{-1}) was used for the preparation of aqueous solutions.

2.2. Preparation of solutions

The phosphate buffered saline (PBS) (50 mM, pH = 7.0) solution was prepared by adjusting the proportion of monobasic sodium phosphate and dibasic sodium phosphate solutions and subsequently adding 0.9% NaCl to the solution. The solution of Ur (1 mg/ml) was freshly prepared in PBS buffer (pH = 7.0). Different concentrations of urea solution (0.83–16.65 mM) were freshly prepared in deionised water.

2.3. Preparation of NiO thin film and immobilization of Ur

Vertically aligned array of 200 nm long NiO nanorods (Nr-NiO) was deposited on ITO coated Corning glass (ITO/Glass) slide using a metal nickel target (99.999% pure) by RF magnetron sputtering technique under the glancing angle deposition (GLAD) configuration at room temperature. The angle between the substrate normal and the direction of incident molecules (target normal) is kept fixed at 70°. ITO/glass slide of 2 cm × 1 cm area was used, out of which half slide (1 cm × 1 cm) was masked prior to the deposition of Nr-NiO for electrical contacts and the remaining area (1 cm × 1 cm) of the slide was having Nr-NiO. 10 μl of urease solution (1.0 mg/ml, in phosphate buffer, 50 mM, pH 7.0) having a low IEP of ~5.0 was successfully immobilized on the surface of the conical tip of NiO nanorods via a physical adsorption technique. The prepared bioelectrode (Ur/Nr-NiO/ITO/glass) was kept overnight for drying. A schematic of the prepared bioelectrode with the possible sensing mechanism is shown in Fig. 1.

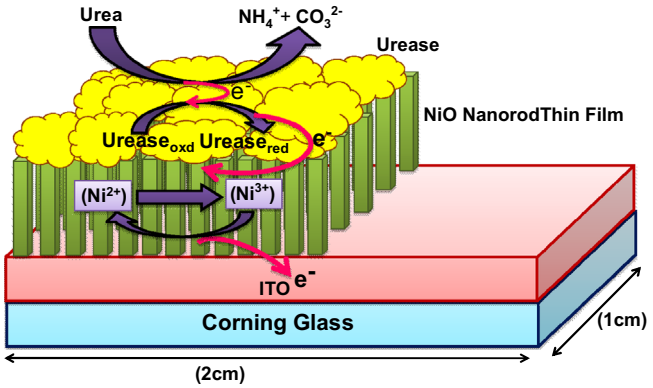

Fig. 1. Schematic of the fabricated Ur/Nr-NiO/ITO/glass bioelectrode.

2.4. Measurement and apparatus

X-ray diffraction (XRD) (Bruker D8 Discover) studies were carried out to identify the crystallographic structure of the prepared array of NiO nanorods. Scanning Electron Microscope (SEM) (Zeiss FESEM) working at 6 KV was used to study the surface morphology of the prepared array of NiO nanorods. The length of Nr-NiO was determined using SEM and surface profiler (Dektak 150). A Fourier transform infrared (FTIR) (PerkinElmer, Model: Frontier) spectrophotometer was used to characterize the NiO nanorods and to confirm the immobilization of urease on its surface. Electrochemical analysis was conducted on a Gamry Reference 600 Potentiostat/Galvanostat using a conventional three-electrode cell configuration with Ag/AgCl serving as reference electrode, platinum foil as counter electrode and prepared bioelectrode as a working electrode in a phosphate buffered saline (PBS) solution (50 mM, pH 7.0, 0.9% NaCl) without any external mediator. The apparent enzyme activity of the bioelectrode was studied using a UV–vis spectrophotometer (PerkinElmer, Lambda 35).

3. Results and discussion

3.1. Structural and morphological studies

Fig. 2(a) shows the XRD pattern of the array of NiO nanorod deposited under GLAD configuration at room temperature on ITO coated glass slide. The XRD pattern exhibits a single peak at $2\theta \approx 42.82°$ corresponding to the (200) reflection of the cubic (fcc) phase of NiO indicating the growth of a preferred a-axis oriented single phase NiO nanorods. The estimated value of '*a*' is found to be about 4.22 Å (space group: *Fm*3*m*) which is higher than the corresponding bulk value (4.177 Å) of NiO [JCPDS 47-1049]. The observed results indicate an expansion in the unit

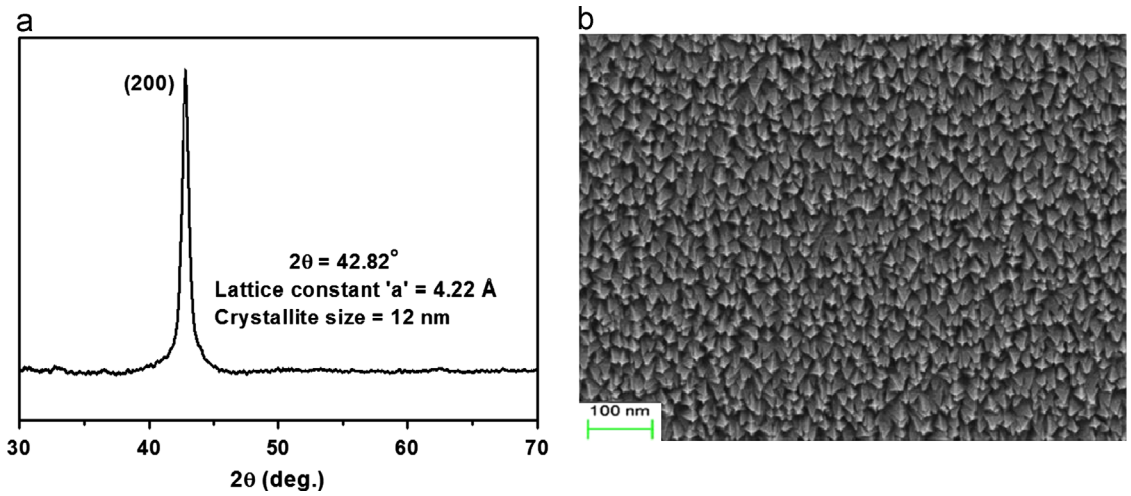

Fig. 2. (a) X-ray diffraction pattern of the thin film of NiO nanorods and (b) Scanning Electron Microscopic (SEM) image of the thin film of NiO nanorods.

cell of prepared NiO nanorods along the '*a*' axis and is associated with the presence of tensile stress in the Nr-NiO. The crystallite size of the NiO nanorods calculated from the (200) XRD peak using the Debye–Scherrer formula is found to be about 12 nm.

Fig. 2(b) shows the SEM microimages of the top surface of the array of NiO nanorods grown on ITO/glass. From Fig. 2(b) it is clearly revealed that the closely packed and well isolated array of vertically aligned NiO nanorods are grow on the surface of ITO/glass slide with conical shaped tips, and thus provided higher surface area to volume ratio. The average diameter of synthesized nanorods from SEM study is estimated to be around 10 nm and is in good agreement with the XRD results. The nanorods are found to be uniformly distributed on the surface of ITO coated glass slide with nanopores in between (Fig. 2(b)). The rough surface morphology of the prepared array of closely packed nanorods is advantageous for higher loading of the immobilized enzyme (urease) and hence is expected to yield enhanced biosensing response characteristics.

3.2. FTIR spectroscopy

NiO nanorods synthesized on ITO/glass slide using GLAD is characterized by FTIR spectroscopy in the range of 400–2000 cm^{-1} before and after immobilization of enzyme (urease) and the corresponding spectra are shown in Supplementary Fig. 1 (a). The absorption bands observed at around 664 and 463 cm^{-1} (Suppl. Fig. 1(a)) are assigned to the stretching vibration and the torsional vibration modes of the Ni–O bond at the tetrahedral and the octahedral sites, respectively (Arora et al., 2011). The band at 576 cm^{-1} corresponds to the stretching mode of the Ni–O–Ni bond (Arora et al., 2011). The band observed at 1150 cm^{-1} is attributed to the stretching vibration mode of the hydroxyl group (Arora et al., 2011). The absorption band observed at 1636 cm^{-1} corresponds to bending mode of the O–H group, which is associated with the adsorbed water molecules on the surface of Nr-NiO.

The binding of the enzyme (urease) onto the surface of Nr-NiO/ITO/glass electrode is revealed by the appearance of additional absorption bands at around 1100 cm^{-1}, 1440 cm^{-1} and 1661 cm^{-1} as shown in Suppl. Fig. 1(a). The absorption band at 1100 cm^{-1} corresponds to the C–O stretching due to amide band in proteins. The bands observed at 1440 cm^{-1} and 1661 cm^{-1} are attributed to the C–N axial deformation (amine group band) and N–H deformation mode in amide II respectively (Kaushik et al., 2009; Ali et al., 2009). The observed results confirm the successful immobilization of urease on the surface of conical tips of NiO nanorods.

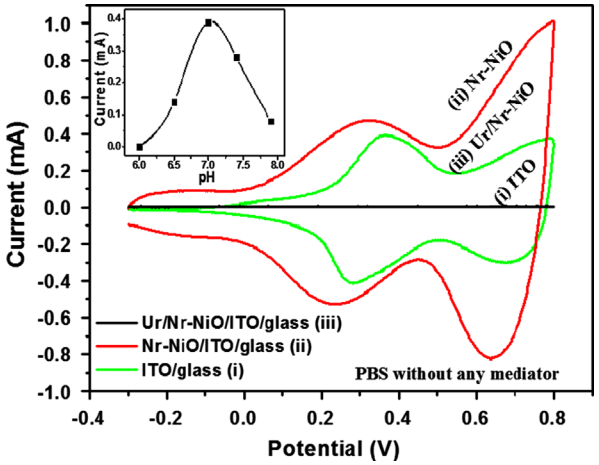

Fig. 3. Cyclic voltammogram of the ITO/glass (curve i), Nr-NiO/ITO/glass electrode (curve ii) and Ur/Nr-NiO/ITO/glass bioelectrode (curve iii) in a PBS buffer without any external mediator. Inset shows the effect of pH of PBS on the peak oxidation current of the Ur/Nr-NiO/ITO/glass bioelectrode.

3.3. Biosensing response characteristics

Biosensing response characteristics of the prepared Ur/Nr-NiO/ITO/Glass bioelectrode towards urea have been investigated using cyclic voltametric (CV) studies. Fig. 3 shows the cyclic voltammetric (CV) spectra of the (i) ITO/glass slide (ii) Nr-NiO/ITO/glass electrode and (iii) Ur/Nr-NiO/ITO/glass bioelectrode in a PBS solution without any external mediating agent.

It may be seen from Fig. 3 that the ITO/glass electrode does not show any oxidation or reduction peaks (curve (i) in Fig. 3) over the entire measured potential window (−0.3 V to 0.8 V) due to the absence of any redox couple in the electrolyte or in the electrode. On the other side, Nr-NiO/ITO/glass electrode shows well defined oxidation and reduction peaks in the CV spectra (curve (ii) in Fig. 3) using the same electrolyte without having any external mediator. The observed results clearly shows that the synthesized NiO nanorods possess the redox couple ($Ni^{2+} \leftrightarrow Ni^{3+}$) giving the redox peaks in the CV spectra of Nr-NiO/ITO/glass electrode (curve (ii) in Fig. 3). The value of peak oxidation current obtained for the Nr-NiO/ITO/glass electrode is found to be about 485 uA at a relatively lower potential (~0.32 V). The separation between the peak oxidation and peak reduction currents (curve (ii) in Fig. 3) is very small (0.09 V) indicating fast electron communication trough the fabricated electrode (Nr-NiO/ITO/glass). The magnitude of peak

oxidation current is found to decrease considerably (394 μA) on immobilization of urease on the surface of the prepared Nr-NiO/ITO/glass electrode. The observed decrease in peak oxidation current is owing to the non-conducting nature of the urease immobilized on the electrode surface, which hinders the interfacial electron transfer. Since the activity of the enzyme (urease) is highly sensitive to the pH of the supporting electrolyte, influence of pH of the electrolyte on the response of the prepared bio-electrode (Ur/Nr-NiO/ITO/glass) was investigated in order to ascertain the optimal working conditions. The variation of peak oxidation current obtained for the bioelectrode as a function of the varying pH of the PBS solution is shown in the inset of Fig. 3. It may be seen from the inset of Fig. 3 that the bioelectrode shows maximum peak oxidation current and hence a maximum activity at a pH of 7.0. Thus, pH of the PBS solution is maintained at 7.0 for rest of the experiments.

In order to further analyze the kinetic and transfer characteristics of the prepared Ur/Nr-NiO/ITO/glass bioelectrode, CV measurements were carried out as a function of scan rate (v) from 100 to 180 mV/s as shown in Fig. 4.

It is interesting to note from Fig. 4 that with increase in scan rate, the separation between the oxidation (E_{po}) and reduction peak potential (E_{pr}) for the bio-electrode increases continuously implying the quasi-reversible behavior of the system (Matharu et al., 2009). The peak oxidation (I_{po}) and reduction (I_{pr}) currents varies linearly with the square root of scan rate (inset of Fig. 4), indicating that the electrochemical process taking place at the bio-electrode (Ur/Nr-NiO/ITO/glass) is diffusion controlled (Arora et al., 2011).

The surface concentration of the ionic species (I^*) on the Ur/Nr-NiO/ITO/glass bioelectrode is estimated using the Brown–Anson model based on the following equation (Arora et al., 2011):

$$I_{pa} = \frac{n^2 F^2 I^* s v}{4RT} \quad (1)$$

where n is the number of electrons transferred (1 in the present case), F is the Faraday constant (96485 C/mol), R is the gas constant (8.314 J mol^{-1} K^{-1}), s is the surface area of the bioelectrode (1 cm^2), v is scan rate, and T is the temperature (300 K). The estimated value of the surface concentration of the ionic species (I^*) on the Ur/Nr-NiO/ITO/glass bioelectrode is about 9.1×10^{-7} mol cm^{-2}. Such a high value of surface concentration reveals that a large numbers of ionic species are available on the surface of prepared bioelectrode for oxidation, leading to higher redox current. The higher surface concentration of ionic species is attributed to the presence of closely packed NiO nanorods based NiO matrix in the prepared bioelectrode. The amperometric biosensing response of prepared Ur/Nr-NiO/ITO/glass bioelectrode were obtained as a function of the urea concentrations from 0.83 to 16.65 mM (physiological range = 1.33–3.33 mM), and are shown in Fig. 5.

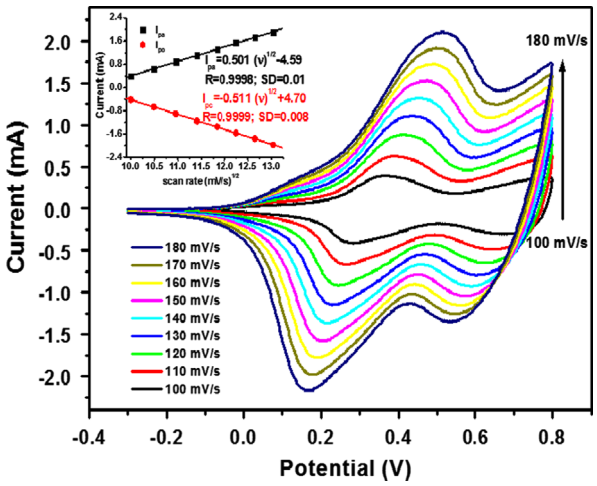

Fig. 4. CV spectra of Ur/Nr-NiO/ITO/glass bio-electrode in PBS solution obtained at different scan rate varied from 100 to 180 mV/s. Inset gives the variation in oxidation (I_{po}) and reduction peak currents (I_{pr}) as a function of (scan rate)$^{1/2}$.

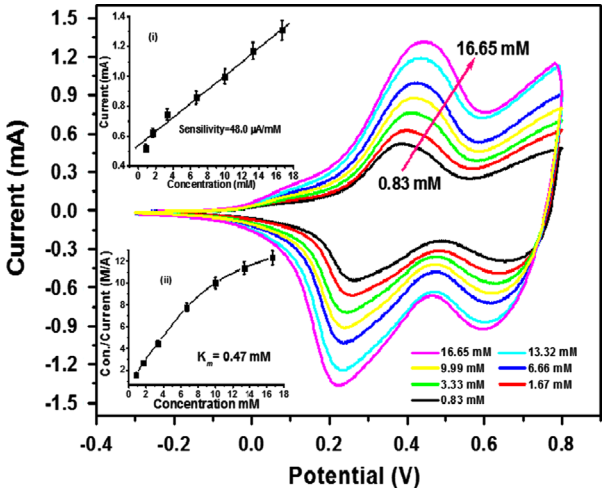

Fig. 5. Amperometric response of the Ur/Nr-NiO/ITO/glass bioelectrode as a function of urea concentration (0.83–16.65 mM). Inset shows (i) variation of the peak oxidation current as a function of urea concentration and (ii) Hanes plot between the analyte concentration and analyte concentration/current.

The peak oxidation and reduction current were found to increase continuously with successive addition of urea in the PBS solution without using any external mediator (Fig. 5). The linear increase in the peak oxidation and reduction current with increase in the urea concentration as shown in Fig. 5 can be understood by the bio-chemical reaction involved in the sensing response of the prepared biosensor (Ur/Nr-NiO/ITO/glass). The schematic of the possible biochemical reaction occurring at Ur/Nr-NiO/ITO/glass bio-electrode is shown in Fig. 1. The immobilized urease on the surface of prepared bioelectrode hydrolysis the analyte (urea) in the solution and in this process the thiol group present at the active sites gets oxidized rendering the enzyme inactive. The enzyme activity is regained by reduction to normal thiol form via exchange of electron through the Nr-NiO matrix. The reduced thiol group in urease donates the excess electron to the Nr-NiO matrix to reduce the redox species (Ni^{3+} to Ni^{2+}). The Nr-NiO matrix reoxidizes (Ni^{2+} to Ni^{3+}) by transferring the electron to the external circuit due to efficient electron communication and good redox property of prepared NiO nanorods based bio-matrix. Whereas, during the reverse cycle of the voltammogram the process repeats in an opposite manner. Hence, catalytic oxidation of the thiol group of urease involves gain or loss of electrons from Nr-NiO matrix thus completing a redox reaction. The observed linear increase in oxidation and reduction currents with increasing concentration of urea is attributed to the increase in the number of loss and gain of electrons during oxidation and reduction of urea respectively. This may be attributed to the fact that NiO nanorods provide large surface to volume ratio for efficient loading of enzyme and act as good acceptors of the electrons generated during reoxidation of immobilized Ur. These electrons are transferred to underneath ITO electrode via the Ni^{+2}/Ni^{+3} redox couple of NiO nanorods, resulting in an increased electrochemical current response. The magnitude of peak oxidation current was found to increase linearly from 0.52 mA to 1.31 mA with an increase in the urea concentration from 0.83 mM to 16.65 mM in reagent free PBS

buffer [inset (i) in Fig. 5] and follows regression equation:

$$\text{Peak current (mA)} = 0.048 \times \text{urea concentration (mM)} + 0.535 \quad (R = 0.997,\ \text{S.D.} = 0.019\ \text{mA}) \qquad (2)$$

In order to confirm the fact that immobilized urease is responsible for the catalytic current in the presence of analyte (urea), a control experiment was carried out in which CV response of Nr-NiO/ITO electrode without immobilization of urease on Nr-NiO/ITO/glass electrode was studied as a function of urea concentration. No significant changes in oxidation and reduction currents were observed in the CV scan with urea concentration over a wide range from 0.83 to 16.65 mM indicating that the oxidation of urea does not occur directly on the surface of the Nr-NiO matrix without having urease. Thus, the observed increase in oxidation current in the biosensing reaction involving Ur/NiO-NPs/ITO/glass bio-electrode with urea concentrations (Fig. 5) is due to the bio-electrocatalytic oxidation of urea; only in the presence of immobilized urease on the surface of Nr-NiO matrix. Furthermore, in order to understand the selectivity of the prepared biosensor, the electrochemical response of both Nr-NiO/ITO and Ur/Nr-NiO/ITO in the presence and absence of NH^{4+} in PBS solution has been studied. No appreciable change in the electrochemical response of the Nr-NiO/ITO/glass electrode is observed in the presence and absence of NH^{4+}. However, as discussed earlier, the oxidation current decreases after immobilization of Ur on the Nr-NiO/ITO electrode as shown in Fig. 3. But no change in the electrochemical response of Ur/Nr-NiO/ITO bioelectrode is also observed in the presence and absence of NH^{4+}. This clearly indicates that the change in oxidation and reduction current for Ur/Nr-NiO/ITO/glass bioelectrode with urea concentration is not due to the presence of NH^{4+} ions in the PBS buffer. However, the observed change in oxidation and reduction current (Fig. 5) is attributed to the oxidation and subsequent reduction of the thiol group present at the active sites of the immobilized urease which is activated during the hydrolysis of urea (analyte) (Uchiyama et al., 2002).

The sensitivity of the prepared biosensor towards urea has been calculated from the slope of the calibration curve (inset (i) in Fig. 5) and is found to be about 48 μA/mM. The sensitivity obtained for the prepared bioelectrode (Ur/Nr-NiO/ITO/Glass) is much higher in comparison to the corresponding results reported for other metal oxides and, polymer membrane based urea biosensors such as Rhodium on PAN membranes—1.85 μA/(mM) (Velichkova et al., 2011), nanostructured polymer membrane—3.19 μA/(mM) (Gabrovska et al., 2011), poly(N-glycidylpyrrole-co-pyrrole)—4.5 μA/(mM) (Bozgeyik et al., 2011), Zinc oxide-chitosan nanobiocomposite—0.78 μA/(mM) (Solanki et al., 2008), Zinc oxide nanostructured film—8.64 μA/(mM) (Ali et al., 2009), etc. Recently, we have studied the biosensing response of NiO nanoparticles (NPs) based matrix synthesized using chemical route for detection of urea (Tyagi et al., 2013). The sensitivity of the NiO-NPs based biosensor was about 21.33 μA/mM, and is much lower than the corresponding value (48 μA/mM) obtained in the present work in a reagent free PBS buffer for biosensor based on Nr-NiO matrix prepared by GLAD. From the above results it is observed that the NiO nanorods based urea biosensor gives superior electrocatalytic activity and thus enhanced biosensing response characteristics.

In order to evaluate the reproducibility of the fabricated NiO nanorods based bioelectrode, repetitive CV measurements were carried out with the successive addition of urea in PBS. The current measured in repetitive measurements exhibits same response characteristics within an accuracy of ±2%, which highlights the excellent reproducibility of the prepared bio-electrode towards urea. Affinity of the immobilized urease molecules on the tip surface of Nr-NiO matrix towards urea molecules was estimated from Hane's plot [inset (ii) of Fig. 5] by evaluating Michaelis–Menten kinetic parameter (K_m). The estimated value of K_m was found to be about 0.47 mM which is relatively lower than the corresponding values reported by other workers for urea biosensors (Kaushik et al., 2009; Ali et al., 2009; Velichkova et al., 2011; Jia et al., 2011). The low value of K_m obtained in the present study indicates the enhanced activity of urease towards its analyte (urea). Increased interaction between the enzyme's active sites and the analyte is attributed to the favorable conformational changes in the enzyme structure on being immobilized, which are facilitated by the suitable biocompatible microenvironment provided by the Nr-NiO matrix.

3.4. Photometric enzyme assay

The apparent enzyme activity of the Ur/Nr-NiO/ITO/glass bioelectrode has been determined using a photometric enzyme assay. The prepared bioelectrode was dipped for 2 min in 3.17 ml of PBS solution (pH 7.0), containing 10 μl of Nessler's solution and 100 μl of analyte (urea) in varying concentration (0.83–16.65 mM). The difference between the initial and final absorbance of the bioelectrode at a fixed wavelength ($\lambda = 385$ nm), was measured, and the corresponding values are plotted in Supplementary Fig. 2 as a function of urea concentration. The immobilized Ur on the surface of Nr-NiO matrix catalyzes the hydrolysis of urea to produce ammonia, which in turn reacts with Nessler's reagent to form a colored product, $NH_2Hg_2I_3$ thereby resulting in change in absorbance (Tiwari et al., 2009).

The enzyme activity of the bioelectrode increases linearly with increasing concentration of urea up to 8.32 mM (Suppl. Fig. 2) and thereafter showed saturating trend. The apparent enzyme activity, i.e., the amount of enzyme bound on the surface of Nr-NiO matrix has been calculated using the equation $a_{app}^{enz}(\text{U cm}^{-2}) = AV/\varepsilon ts$, where A is the difference in the absorbance before and after incubation of the bioelectrode in the saturated solution, V is the total volume (3.17 cm^3), ε is the millimolar extinction coefficient of Nessler's reagent, t is the reaction time (2 min) and s is the surface area of the prepared bioelectrode (Tiwari et al., 2009). The estimated value of the apparent enzyme activity was found to be about 5.1×10^{-1} U cm^{-2}, which is quite high as compared to the corresponding value [4.3×10^{-1} U cm^{-2}] obtained for NiO nanoparticle based urea biosensor fabricated using chemical route in one of our previous report (Tyagi et al., 2013). The obtained result clearly indicates a higher activity of the immobilized Ur on the surface of Nr-NiO matrix synthesized using GLAD in the present case. The observed high value of apparent enzyme activity is due to the large surface area provided by the vertically align array of NiO nanorods that leads to the higher enzyme loading.

3.5. Stability study

Fast degradation of the biosensors based on nanostructured matrix is the main concern of the research community. Thus the stability of the prepared bioelectrode (Ur/Nr-NiO/ITO/glass) is investigated over a period of 20 weeks by measuring the electrochemical current response after a regular interval of time (2 weeks). Inset of Suppl. Fig. 2 shows the variation in the peak oxidation current of Ur/Nr-NiO/ITO/glass bio-electrode as a function of time. The prepared bioelectrode retains more than 92% of the response even after 20 weeks when stored at 4 °C, demonstrating the high shelf life of the Nr-NiO based bio-electrode. Shelf life of the prepared biosensor is much higher compared to other bio-electrodes developed for urea biosensing using various matrices such as poly(N-glycidylpyrrole-co-pyrrole) resulted in 40% loss of enzyme activity in 10 days (Bozgeyik et al., 2011), nanostructured polymer membrane showed a shelf life of 10 days (Gabrovska et al., 2011), zirconia (ZrO_2) film, (Sumana et al., 2010), poly (N-3 aminopropyl pyrrole-co-pyrrole), (Rajesh et al., 2005), Functionalized H40-Au nanoparticles (Tiwari et al., 2009) and iron

oxide-chitosan nanobiocomposite (Kaushik et al., 2009) matrices showed a poor shelf life of about 56 days, 60 days, 129 days and 56 days respectively. The shelf life of NiO nanoparticles based urea bioelectrode in our previous study (Tyagi et al., 2013) was also good [16% degradation in response after 20 weeks], however the results in the present study using Nr-NiO matrix are much superior [less than 8% degradation in response after 20 weeks]. The exceptionally high shelf life of the Ur/Nr-NiO/ITO/glass bio-electrode may be attributed to the fact that the array of NiO nanorods are deposited using GLAD under controlled and reproducible processing conditions, leading to high stability and excellent biological compatibility which provided good microenvironment for the enzyme to maintain its bioactivity.

3.6. Selectivity study

Selectivity study of Ur/Nr-NiO/ITO/glass bioelectrode towards urea has also been performed. The CV response was taken after adding normal concentration of urea (1 mM) with different interferants in normal concentrations including glucose (5.6 mM), uric acid (0.1 mM), cholesterol (5 mM), lactic acid (5 mM) and ascorbic acid (0.05 mM).

The Ur/Nr-NiO/ITO/glass bioelectrode shows a maximum interference of about 3.1% in the presence of uric acid and effect of the presence of other interferents with urea is less than 2.0% (Suppl. Fig. 3).

4. Conclusion

Vertically aligned NiO nanorods based bioelectrode has been developed for the realization of a highly sensitive and stable reagentless urea biosensor. The prepared bioelectrode (Ur/Nr-NiO/ITO/glass) exhibits improved linearity over a wide detection range (0.83–16.65 mM), a high sensitivity of about 48.0 μA/(mM), a high apparent enzyme activity of 5.1×10^{-1} U/cm^2, a fast response time of 5 s and a long shelf life of 20 weeks. The low K_m value of 0.47 mM indicates a high affinity of the immobilized urease on the surface Nr-NiO/ITO/glass electrode towards urea. The NiO nanorods provide suitable active surface with its own redox couple ($Ni^{2+}\leftrightarrow Ni^{3+}$) for enhanced urease immobilization, favorable conformation, and fast electron transfer which catalyzes the electrochemical oxidation of urea.

Acknowledgments

The authors are thankful to the department of Science and Technology (DST), Govt. of India for financial support to conduct this research work. One of the authors (MT) acknowledges CSIR and the University of Delhi for research fellowship.

Appendix A. Supplementary data

Supplementary data associated with this article can be found in the online version at http://dx.doi.org/10.1016/j.bios.2013.08.020.

References

Ahuja, T., Kumar, D., Singh, N., Biradar, A.M., Rajesh, 2011. Materials Science and Engineering C 31, 90.
Ali, A., Ansari, A.A., Kaushik, A., Solanki, P.R., Barik, A., Pandey, M.K., Malhotra, B.D., 2009. Materials Letters 63, 2473.
Ansari, S.G., Wahab, R., Ansari, Z.A., Kim, Y.S., Khang, G., Hajry, A.A., 2009. Sensors and Actuators B 137, 566.
Arora, K., Tomar, M., Gupta, V., 2011. Biosensors and Bioelectronics 30, 333.
Batra, N., Tomar, M., Gupta, V., 2012. Analyst 137, 5854.
Bozgeyik, I., Mehmet, S., Emre Çevik, M., Abasıyanık, F., 2011. Current Applied Physics 11, 1083.
Chirizzi, D., Malitesta, C., 2011. Sensors and Actuators B 157, 211.
Das, M., Sumana, G., Nagarajan, R., Malhotra, B.D., 2010. Applied Physics Letters 96, 133703.
Dhawan, G., Sumana, G., Malhotra, B.D., 2009. Biochemical Engineering Journal 44, 42.
Gabrovska, K., Ivanov, J., Vasileva, I., Dimova, N., Godjevargova, T., 2011. International Journal of Biological Macromolecules 48, 620.
Jia, W., Su, L., Lei, Y., 2011. Biosensors and Bioelectronics 30, 158.
Kaushik, A., Solanki, P.R., Ansari, A.A., Sumana, G., Ahmad, S., Malhotra, B.D., 2009. Sensors and Actuators B 138, 572.
Konck, R., Lenarczuk, T., Radomska, A., Glab, S., 2001. Analyst 126, 1080.
Krawczyk, T.K., Moszczynska, M., Trojanowicz, M., 2000. Biosensors and Bioelectronics 15, 681.
Lakard, B., Magnin, D., Deschaume, O., Vanlancker, G., Glinel, K., Champagne, S.D., Nysten, B., Jonas, A.M., Bertrand, P., Yunus, S., 2011. Biosensors and Bioelectronics 26, 4139.
Li, C., Liu, Y., Li, L., Du, Z., Xu, S., Zhang, M., Yin, X., Wang, T., 2008. Talanta **77**, 455.
Matharu, Z., Pandey, P., Pandey, M.K., Gupta, V., Malhotra, B.D., 2009. Electroanalysis 21, 1587.
Rajesh, Bisht, V., Takashima, W., Kaneto, K., 2005. Biomaterials 26, 3683.
Saipina, O.Y., Pyeshkova, V.M., Soldatkin, O.O., Melnik, V.G., Akata, K.B., Walcarius, A., Dzyadevych, S.V., Jafferezic, N.R., 2011. Materials Science and Engineering C 31, 1490.
Sattarahmady, N., Heli, H., Faramarzi, F., 2010. Talanta 82, 1126.
Solanki, P.R., Kaushik, A., Ansari, A.A., Sumana, G., Malhotra, B.D., 2008. Applied Physics Letters 93, 163903.
Sumana, G., Das, M., Srivastava, S., Malhotra, B.D., 2010. Thin Solid Films 519, 1187.
Tiwari, A., Aryal, S., Pilla, S., Gong, S., 2009. Talanta 78, 1401.
Tyagi, M., Tomar, M., Gupta, V., 2012. Analytica Chimica Acta 726, 93.
Tyagi, M., Tomar, M., Gupta, V., 2013. Biosensors and Bioelectronics 41, 110.
Uchiyama, S., Kobayashi, M., Hasebe., Y., 2002. Electroanalysis 14, 1644.
Velichkova, Y., Ivanov, Y., Marinov, I., Ramesh, R., Kamini, N.R., Dimcheva, N., Horozova, E., Godjevargova, T., 2011. Journal of Molecular Catalysis B: Enzymatic 69, 168.
Yang, Z., Si, S., Dai, H., Zhang, C., 2007. Biosensors and Bioelectronics 22, 3283.
Zang, W.D., Jin, C., Chuan, J.L., Xiang, Y.Y., Qi, Z.J., 2010. Mikrochimica Acta 168, 259.